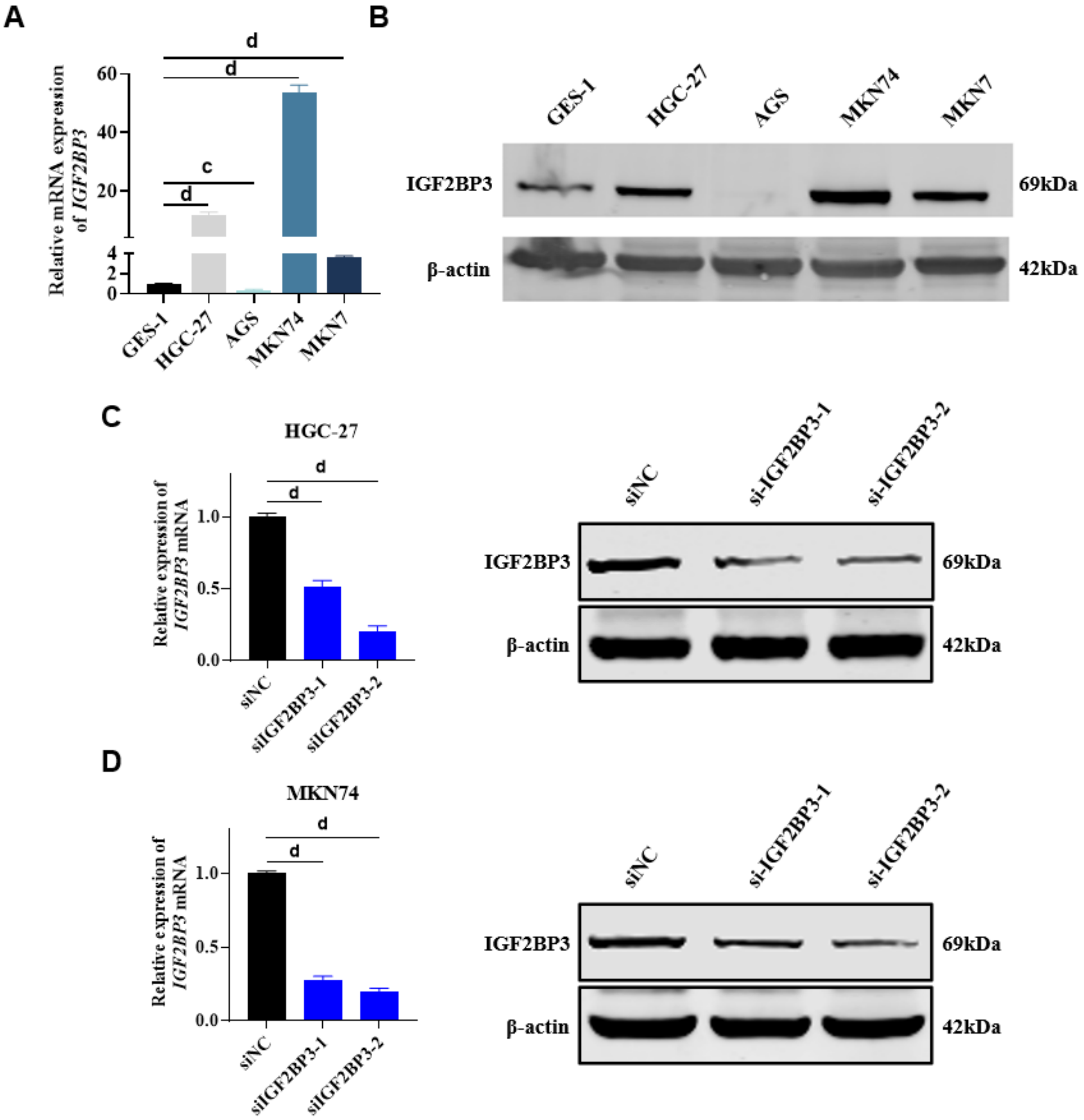

Supplementary Figure 1 Analysis of IGF2BP3 expression and siRNA-IGF2BP3 knockdown efficiency in gastric cell models. A: Expression of *IGF2BP3* mRNA in the GES-1, HGC-27, AGS, MKN74, and MKN7 cell lines; B: Expression of IGF2BP3 protein in the GES-1, HGC-27, AGS, MKN74, and MKN7 cell lines; C: Assessment of siRNA-IGF2BP3 knockdown efficiency in HGC-27 cells by qRT-PCR and WB; D: Assessment of siRNA-IGF2BP3 knockdown efficiency in MKN74 cells by qRT-PCR and WB. Data are presented as the mean ± SD. $^{c}P < 0.001$, $^{d}P < 0.0001$.

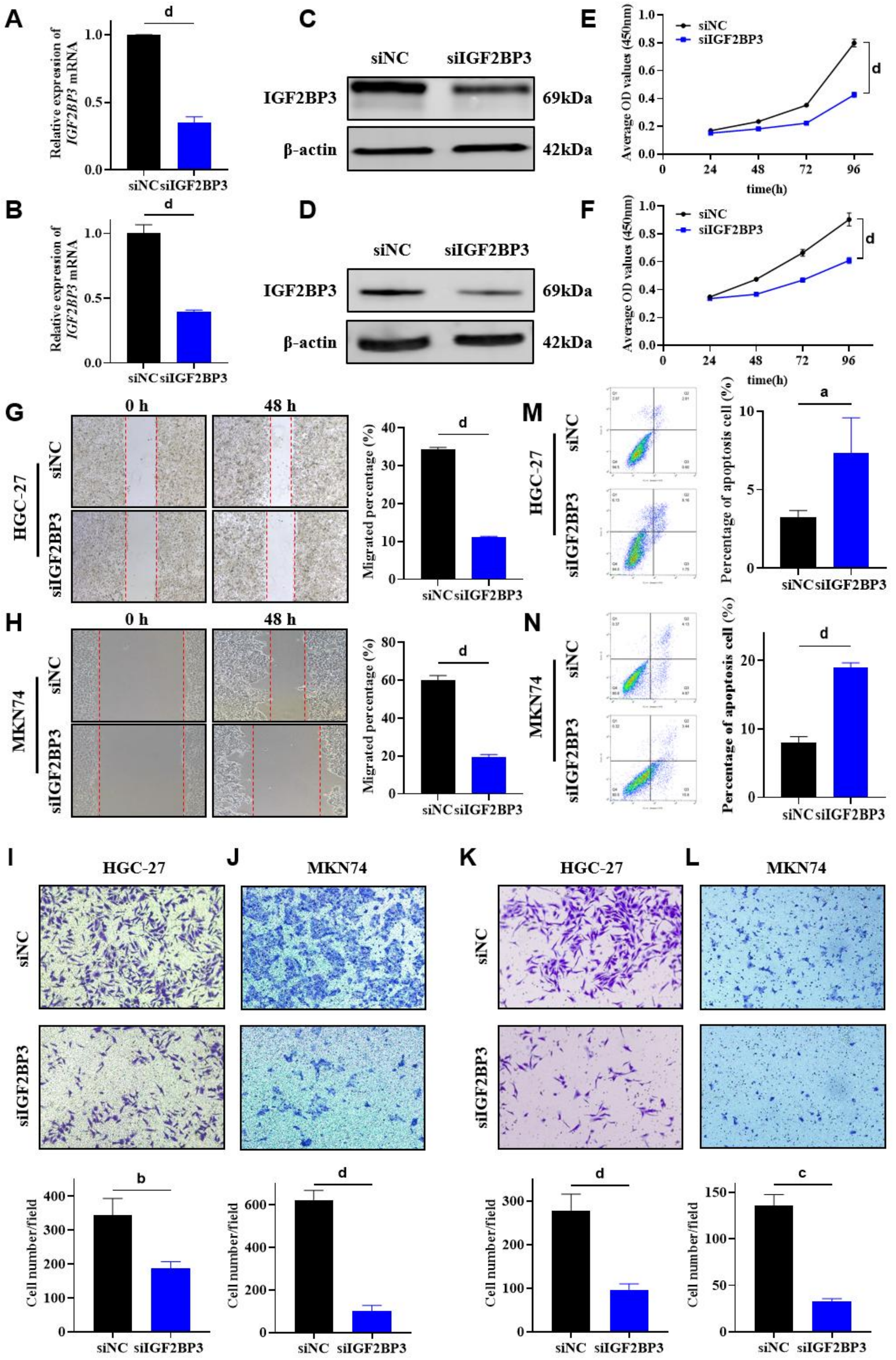

Supplementary Figure 2 Knockdown of IGF2BP3 in GC cells suppresses cell proliferation, migration, and invasion *in vitro*. A, B: Expression of *IGF2BP3* mRNA in HGC-27 and MKN74 cells as detected by qRT-PCR; C, D: Expression of IGF2BP3 protein in HGC-27 and MKN74 as detected by WB; E, F: Effects of IGF2BP3 knockdown on proliferation of HGC-27 and MKN74 cells as determined by CCK-8 assay; G, H: Effects of IGF2BP3 knockdown on migration of HGC-27 and MKN74 cells as assessed by wound healing assay, Scale bar: 200 μm; I, J: Effect of IGF2BP3 knockdown on migration of HGC-27 and MKN74 cells as evaluated using transwell migration assays, Scale bar: 100 μm; K, L: Effects of IGF2BP3 knockdown on invasion of HGC-27 and MKN74 cells as assessed using transwell invasion assays, Scale bar: 100 μm; M, N: Effects of IGF2BP3 knockdown on apoptosis of HGC-27 and MKN74 cells as determined by flow cytometry. Data are presented as the mean ± SD. $^{a}P < 0.05$, $^{b}P < 0.01$, $^{c}P < 0.001$, $^{d}P < 0.0001$.

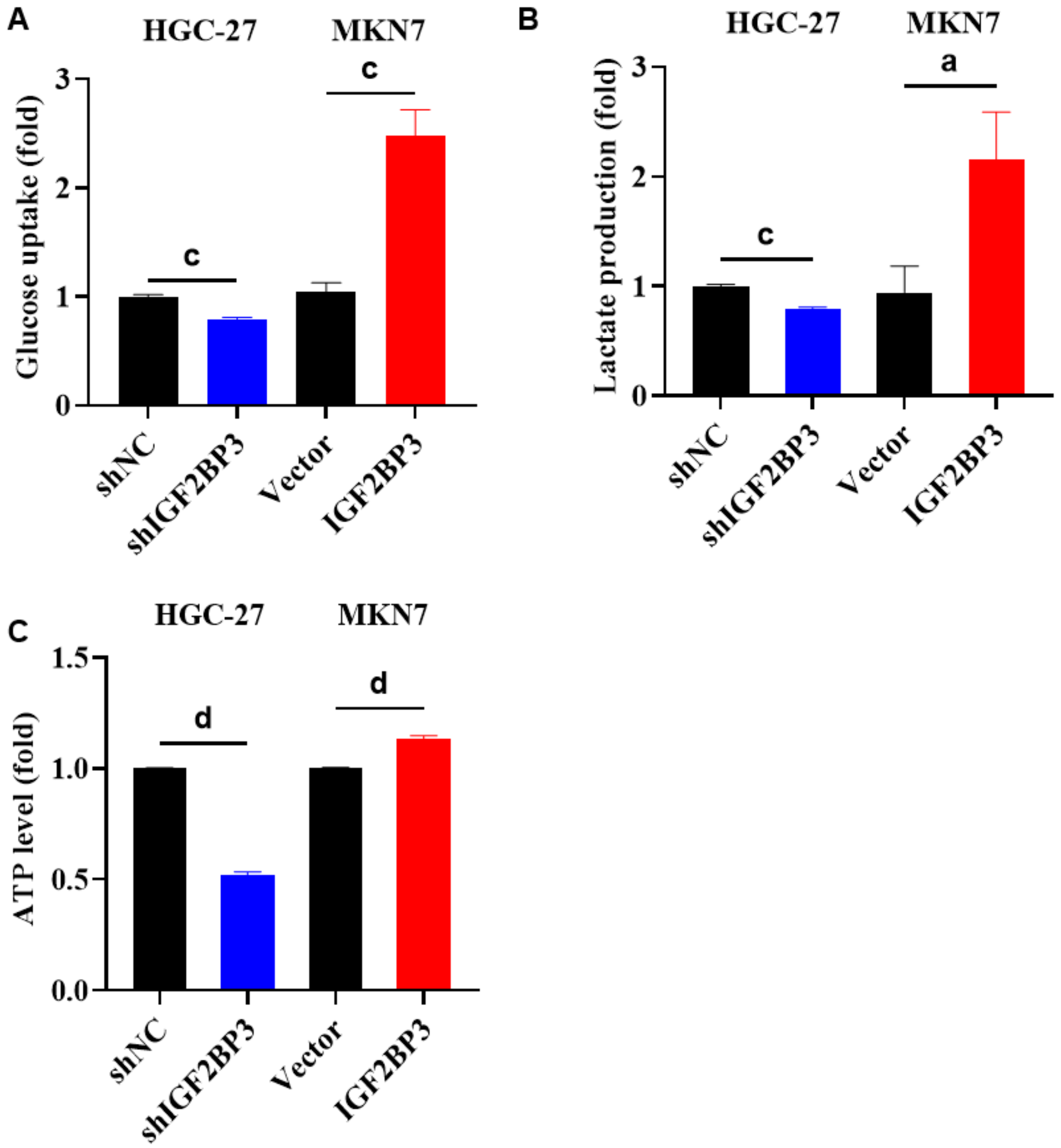

Supplementary Figure 3 IGF2BP3 affects glucose metabolism in GC cell lines. A: Assessment of glucose uptake in GC cells following modulation of IGF2BP3 expression; B: Assessment of lactic acid production in GC cells following modulation of IGF2BP3 expression; C: Assessment of ATP content in GC cells following modulation of IGF2BP3 expression. Data are presented as the mean ± SD. $^{a}P < 0.05$, $^{c}P < 0.001$, $^{d}P < 0.0001$.

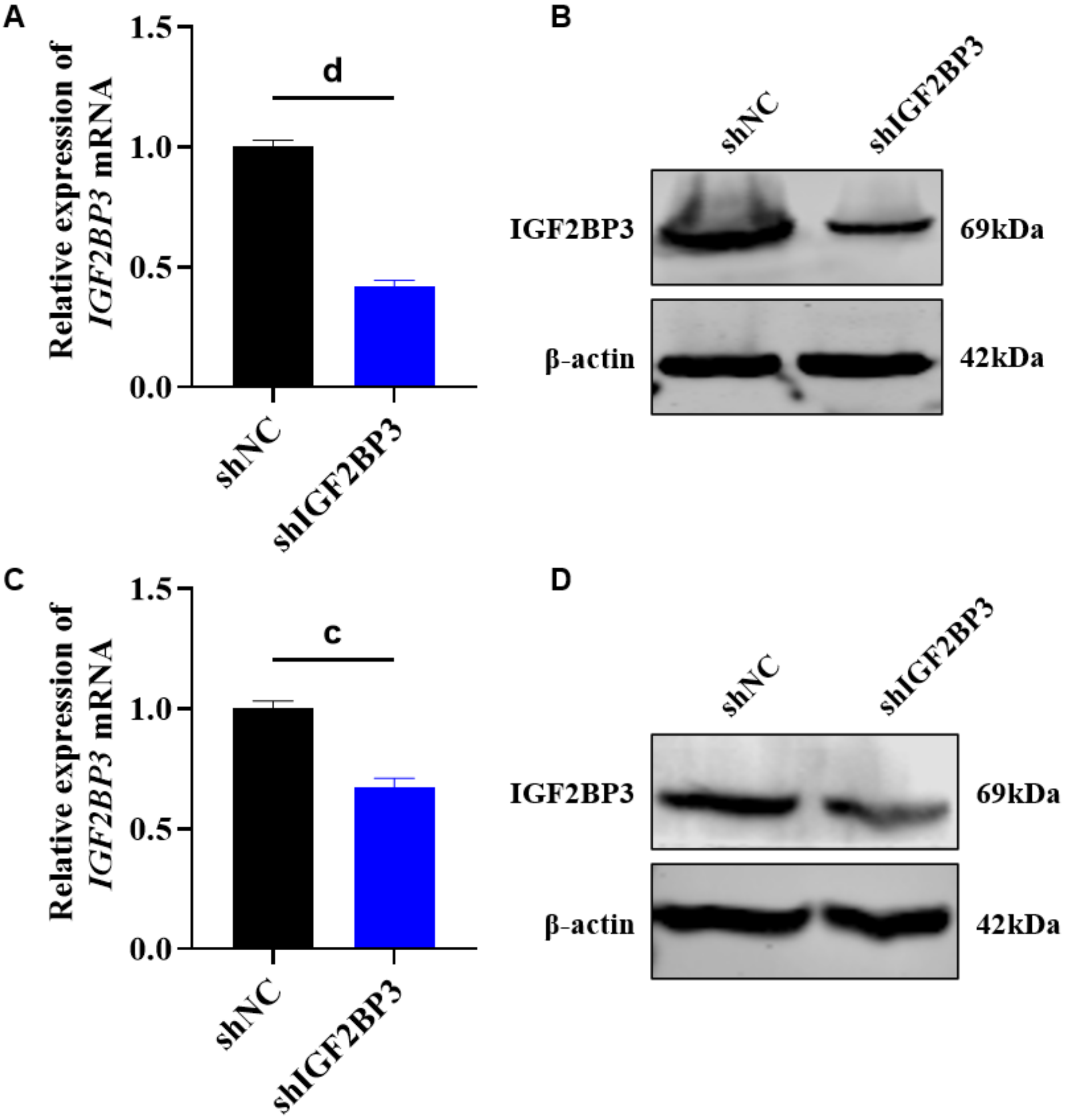

Supplementary Figure 4 Expression of IGF2BP3 in stably transfected cell lines and nude mouse xenografts. A, B: Expression of *IGF2BP3* mRNA (A) and IGF2BP3 protein (B) in control (shNC) and stable IGF2BP3-knockdown (shIGF2BP3) cell lines; C, D: **E**xpression of *IGF2BP3* mRNA (C) and IGF2BP3 protein (D) in nude mouse xenografts from the shNC group and shIGF2BP3 group. Data are presented as the mean ± SD. $^{c}P < 0.001$, $^{d}P < 0.0001$.

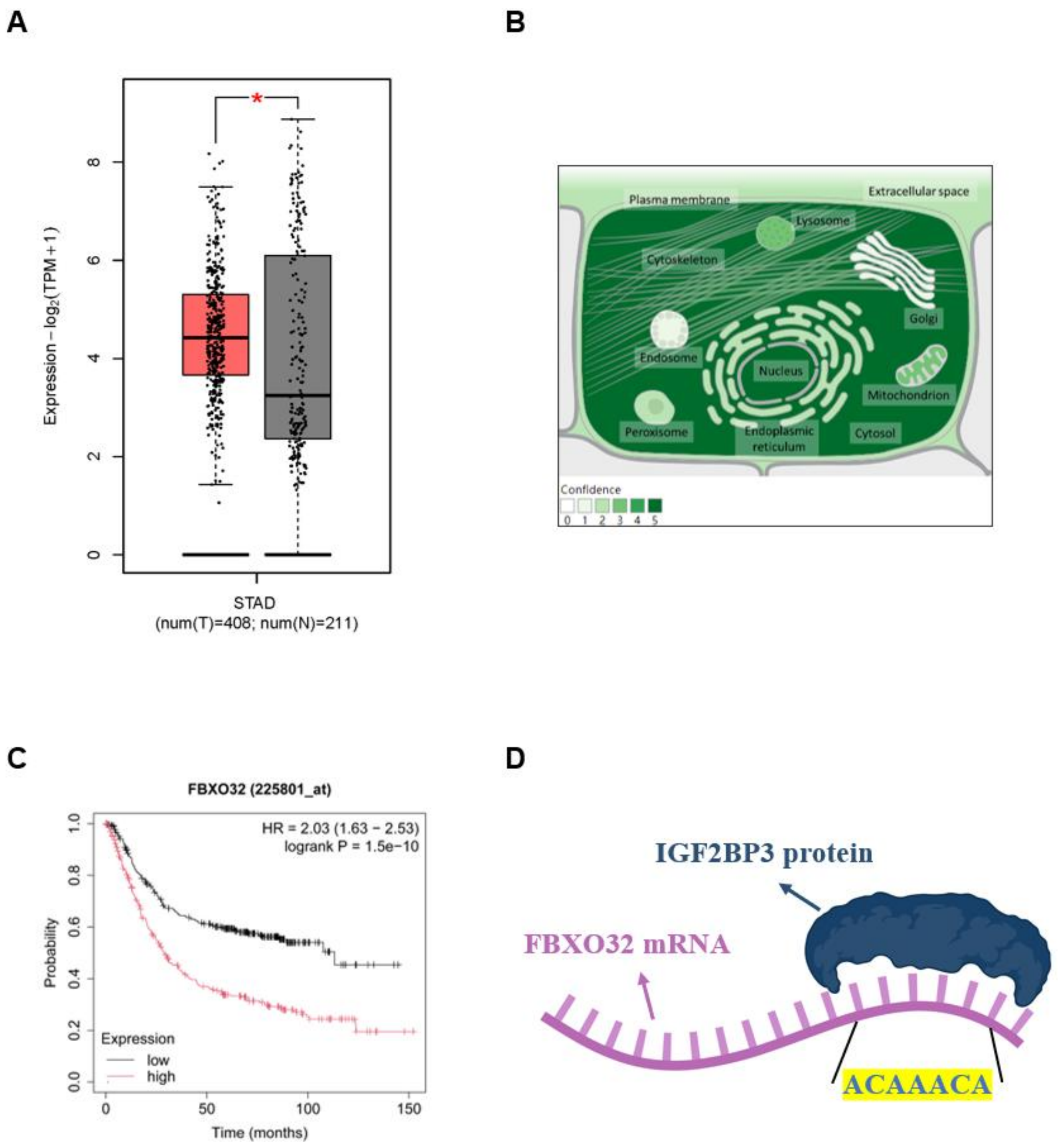

Supplementary Figure 5 Characterization of FBXO32 in GC and prediction of its mRNA binding sites with IGF2BP3 protein. A: Expression of FBXO32 in GC paired tissue cohort from TCGA; B: Subcellular localization of FBXO32 from GeneCards; C: Kaplan–Meier analysis of FBXO32 expression levels and overall survival in patients with GC (The cutoff for high *vs* low expression groups was defined by the median value of FBXO32 expression in the cohort); D: Schematic diagram of catRAPID prediction of the binding site between IGF2BP3 protein and *FBXO32* mRNA.

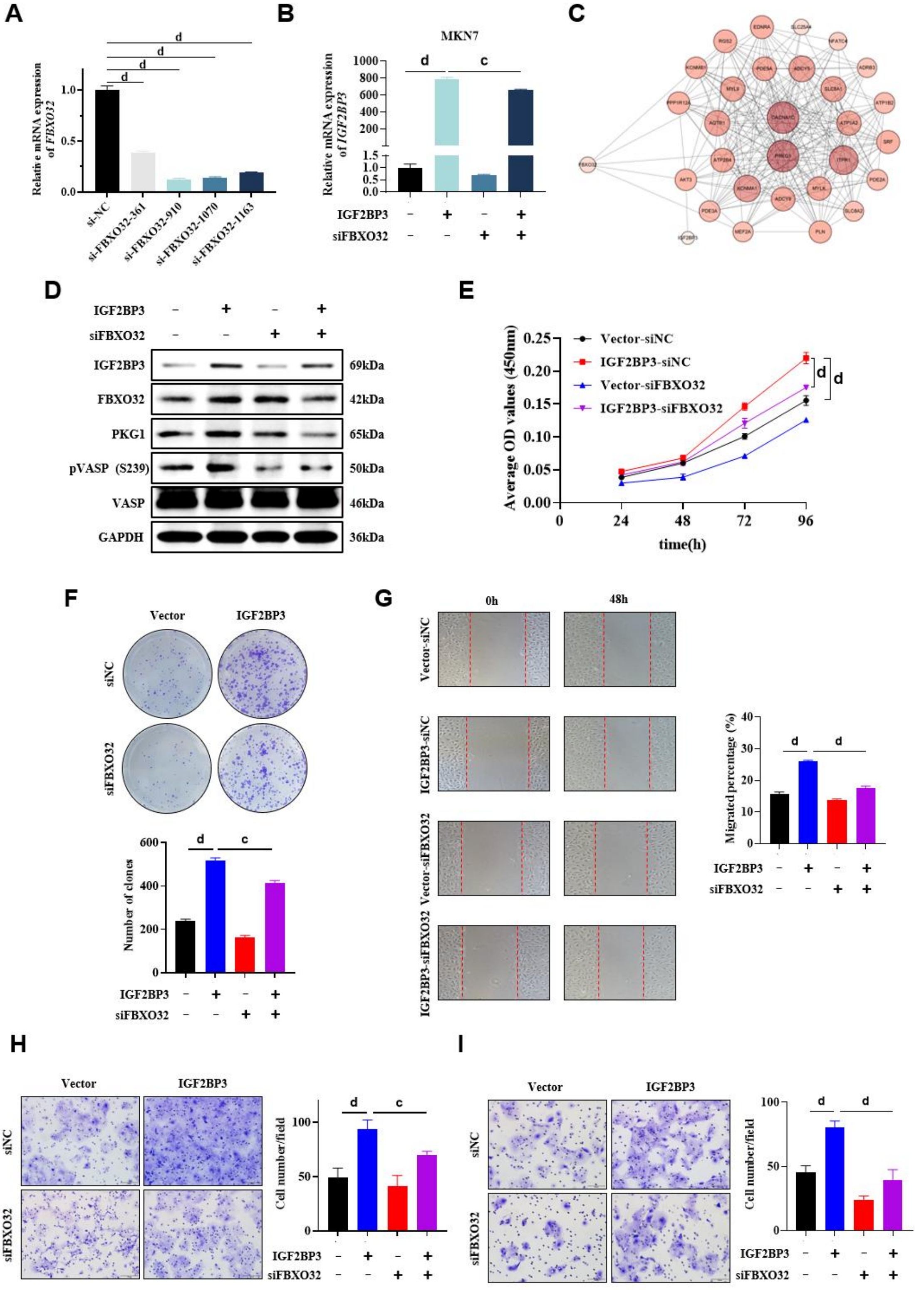

Supplementary Figure 6 The IGF2BP3/FBXO32/cGMP–PKG signaling pathway axis mediates malignant phenotypes in GC. A: Knockdown efficiency of four *FBXO32*-targeting siRNAs in MKN7 cells as assessed by qRT-PCR; B: Expression of *IGF2BP3* mRNA in MKN7 cells as measured by qRT-PCR after co-transfection of pcDNA3.1 (vector) or pcDNA3.1-IGF2BP3 (IGF2BP3) plasmids and siNC or siRNA-FBXO32 (siFBXO32); C: Protein interaction network diagram; D: Expression levels of proteins related to the cGMP–PKG signaling pathway as detected by WB after instantaneous co-transfection of vector/IGF2BP3 and siNC/siFBXO32 in MKN7 cells; E–I: Effects of FBXO32 on IGF2BP3 in MKN7 cells as detected by CCK-8 assay (E), colony formation assay (F), wound healing assay (G) (scale bar: 200 μm), transwell migration assay (H), and transwell invasion assay (I) (scale bar: 100 μm). Data are presented as the mean ± SD. $^{c}P < 0.001$, $^{d}P < 0.0001$.

Supplementary Table 1 Primer sequences for *IGF2BP3*, *FBXO32*, and β-actin

Gene	Forward primer sequence 5′-3′	Reverse primer sequence 5′-3′
IGF2BP3	ACTGCACGGGAAACCCATAG	CCAGCACCTCCCACTGTAAAT
FBXO32	TACGTGGTCCGGCTGTTG	CCATCCGATACACCCACATG
β-actin	CTCCATCCTGGCCTCGCTGT	GCTGTCACCTTCACCGTTCC